European Journal of Wood and Wood Products
https://doi.org/10.1007/s00107-022-01843-1

ORIGINAL ARTICLE

Surface characterization of wood treated with acidic deep eutectic solvents

Ahmet Emre ÇELİK[1] · **Ahmet CAN**[1]

Received: 12 August 2021 / Accepted: 16 May 2022

Abstract

This study investigated the use of deep eutectic solvents (DESs) to improve the accelerated weathering performance of Scots pine (*Pinus sylvestris* L.) wood. In addition to being natural and easily obtained, the simple preparation of these solvents via heating and mixing has led to their use in a pretreatment process. The DES solutions were prepared by mixing, in different molar ratios, oxalic acid (OA) and acetic acid (AA) as hydrogen bond donors (HBDs) and choline chloride (ChCl) and betaine (BT) as hydrogen bond acceptors (HBAs). In this study, the novel DESs were prepared and characterized. Scots pine wood samples prepared in dimensions of 15 (radial) × 75 (tangential) × 150 (longitudinal) mm were treated with the DES solutions at 150 °C for 2 h. The weathering effects on the surface characteristics and morphology of the samples were examined by means of Fourier transform infrared (FTIR) spectroscopy, scanning electron microscopy (SEM), and measurement of color, gloss, and surface roughness. Weathering was carried out via cycles of 8-h UV-light irradiation and 15-min water spraying followed by 3.45-h conditioning in an accelerated weathering test cycle chamber. According to the FTIR results, the lignin ratio decreased significantly in the wood samples subjected to 2-h pretreatment at 150 °C. The results showed that the greatest color change occurred on the surfaces of the control samples, whereas the least color change was observed up to 168 h on the OA-BT samples. The glossiness values increased with the first 168 h of weathering. Thereafter, the gloss values of the samples treated with OA-BT and OA-ChCl remained stable. The surface roughness and degradation of surface components rose with the increase in the weathering exposure period. In accordance with the color and surface roughness measurements, the FTIR spectra proved that for all specimens, lignin continued to degrade on the exposed surfaces throughout 168 h of accelerating weathering.

1 Introduction

Wood, as a renewable lignocellulosic material, is the most suitable material for building construction due to its high strength in proportion to its weight and because of its low processing costs. Lignocellulosic resources, which are rich in cellulose, hemicellulose, and lignin, are the most widely distributed and abundant renewable resources on earth (Sinclair et al. 2018). The major chemical component of a living tree is water; however, on a dry-weight basis, all wood cell walls consist mainly of sugar-based polymers (carbohydrates, 65–75%) that are combined with lignin (18–35%) (Rowell et al. 2005).

Lignin is a renewable and sustainable aromatic feedstock material, corresponding to ~30 wt% of the organic carbon in the biosphere (Boerjan et al. 2003). Lignin is present in the cell walls of lignocellulosic materials as a hydrophobic structural component and plays an important role in the strengthening and impermeabilization of the vegetable tissues (Faruk and Sain 2015). Wood has the highest proportion of lignin (~15–30 wt%) compared to other material types (Upton and Kasko 2016), for example, corn cobs and rice straw contain 3–25% lignin by weight (Smolarski 2012). Lignin content varies among species as well

---

✉ Ahmet CAN
acan@bartin.edu.tr

[1] Forest Industry Engineering, Faculty of Forestry, Bartin University, Bartın, Turkey

as within species. For example, it can range from 25% by weight for *Pinus monticola* to up to 30% for *Pinus palustris* (Mahmood et al. 2018), whereas the species *Pinus sylvestris* contains 19.8% lignin by weight (Cox et al. 2001). When wood is exposed to the outdoor environment, a complex combination of chemical, mechanical, and energy factors causes weathering (Fengel and Wegener 2011). Exposure of wood to UV-light is known to be mainly responsible for the degradation and discoloration of wood surfaces in natural weathering (Müller et al. 2003). Lignin is composed of phenylpropane units and is the main UV-light-absorbing component in wood (20–30%). Most free radicals are produced in the phenolic lignin groups, which are then easily converted into quinonoid structures. It has also been observed that the carbon-carbon bonds adjacent to the α-carbonyl groups in lignin undergo photodegradation via the Norrish Type I reaction (Hon and Shiraishi 2001). The gradual destruction of lignin aromaticity and the formation of carbonyl structures are well-known changes caused by weathering conditions. The increase in the cellulose content of a weathered wood surface was reported to result from the degradation and dissolution of lignin, and vanillin and vanillic acid were found to form as the main components in the degradation of the lignin (Holmbom et al. 1992).

If a safe, low-tech method could be discovered for separating lignin and converting it to another bio product, the increased density of the holocellulose and remaining products could be utilized. After decomposition, lignin could then be converted into valuable fuels and chemicals using existing technology. On the other hand, wood with a reduced lignin ratio but rich in cellulose and hemicellulose is thought to exhibit increased surface resistance against UV rays.

As sustainable alternatives to ionic liquids, deep eutectic solvents (DESs) derived from natural and renewable components are promising as solvents for delignification, with high yields of 58–78% (Alvarez-Vasco et al. 2016). Compared to the traditional alkaline methods, DES pretreatments have resulted in a greater enhancement of digestibility, lower energy consumption, and simpler lignin purification. These solvents are environmentally friendly, easy to prepare, biodegradable and biocompatible, and employ simpler purification and solvent recovery procedures (Gunny et al. 2015). A DES is a eutectic mixture consisting of a hydrogen bond acceptor (HBA) with a hydrogen bond donor (HBD). Choline chloride is a common salt used as the main ingredient in a wide range of available DESs (Abbott et al. 2003; Perez-Sanchez et al. 2013). In addition, betaine also is a cheap natural resource (Perez-Sanchez et al. 2013) that is biodegradable, non-toxic, and can be extracted from sugar beets (Yang et al. 2015). Thus, betaine-based DESs have extensive application possibilities.

The solubility of lignin in DES mixtures provides a new alternative for biomass pretreatment under mild conditions. Recent studies focused on DESs have provided a new perspective on their potential application to lignin extraction (Alvarez-Vasco et al. 2016; Morais et al. 2020; Li et al. 2021). Studies have demonstrated that DES may have a unique potential to dissolve lignin from plant materials (Francisco et al. 2012; Liu et al. 2012). Studies using varied ratios of HBD (choline chloride and betaine) and HBA (oxalic acid and lactic acid) in DES mixtures have shown that they have a significant effect on lignin solubility at different temperatures (Francisco et al. 2012; Alvarez-Vasco et al. 2016; Zhang et al. 2016; Lynam et al. 2017; Tian et al. 2017). In a recent study by Zhang et al. (2016), three kinds of deep DESs, including monocarboxylic acid/choline chloride, dicarboxylic acid/choline chloride, and polyalcohol/ choline chloride, were easily prepared and used in the pretreatment of corncobs. The acid amount, acid strength, and the nature of the HBAs exerted great influence on the pretreatment results. Maximum delignification of 98.5% was observed with ChCl/oxalic acid (Zhang et al. 2016). A DES composed of oxalic acid (dihydrate) was used in lignin extraction from wood biomass with high efficiency (90%) by heating at 110 °C for 9 h (Liu et al. 2017). In another study conducted by Alvarez-Vasco et al. (2016), the delignification efficiency for poplar (hardwood) and Douglas fir (softwood) species was compared. By applying choline chloride-lactic acid DESs at 145 °C for 6 h, 78% of the lignin was removed from the poplar and 58% from the Douglas fir (Alvarez-Vasco et al. 2016). Most of the research conducted with DESs is aimed at using them to transform lignocellulosic materials into more valuable products. Studies using wood have concentrated on lignin solubilization and wood delignification, enzymatic hydrolysis and lignin valorization, and solubilizing cellulose and hemicellulose (Alvarez-Vasco et al. 2016; Lynam et al. 2017; Malaeke et al. 2018; Kim et al. 2018).

Although DESs have been employed in biomass fractionation, to the best of the authors` knowledge, pretreatment of Scots pine (*Pinus sylvestris*) wood for lignin extraction using acidic DESs has not been previously reported. In this work, two acids (oxalic acid and acetic acid) were used as HBDs, and choline chloride and betaine as HBAs. The goal of this research was to investigate the feasibility of this novel approach via accelerated weathering of the wood. In addition to being natural and easily obtained, the simple preparation of DESs via heating and mixing led to their use in the pretreatment process. Color, brightness, and surface roughness measurements and Fourier transform infrared (FTIR) analyses were performed on the samples before and after the pretreatment process, and the changes were examined. In addition, the accelerated weathering effect was investigated

Table 1 DES hydrogen bond donors (HBDs), hydrogen bond acceptors (HBAs), molar ratios, temperatures, and physicochemical property parameters

DESs combination	HBA	HBD	Molar ratio	Temperature (°C)	Density (g/cm^3)	Viscosity (Pa.s)	
						25 °C	150 °C
AA-ChCl	Acetic acid	ChCl	2:1	70	1.21	0.045	0.004
AA-BT		Betaine	1:1	70	1.24	0.320	0.010
OA-ChCl	Oxalic acid	ChCl	1:1.5	90	1.29	0.120	0.006
OA-BT		Betaine	2:1	60	1.31	0.895	0.025

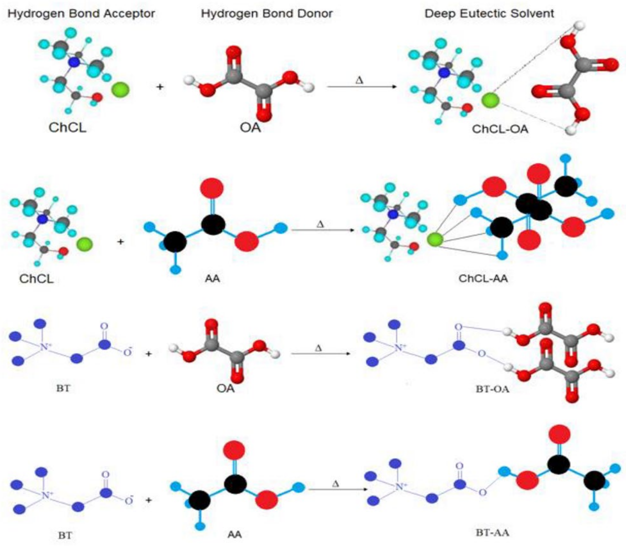

Fig. 1 Synthesis of DESs

by exposing test and control samples to accelerated outdoor conditions according to ASTM G154 (2006) standard for 100, 250, 500, and 1000 h.

2 Materials and methods

2.1 Material

The pine (*Pinus sylvestris* L.) wood was selected from boards cut entirely from sapwood, and specimens (density 0.42 g/cm^3) were prepared in dimensions of 15 (radial, R) × 75 (tangential, T) × 150 (longitudinal, L) mm for the weathering tests.

Choline chloride (ChCl) (99%, 139.62 g/mol, Acros), betaine anhydrous (BT) (98%, abcr), oxalic acid (OA) (126.07 g/mol, Merck), and acetic acid (AA) (60.05 g/mol, Merck) were used as received. The chemical structure of the DES components is shown in Figure S1 in Supplementary Information.

2.2 DESs preparation

Several DESs were prepared by combining OA and AA with ChCl and BT. The components were weighed according to the respective molar ratios (Table 1). The mixtures were stirred with a magnetic stirrer in a water bath at different temperature and atmospheric pressure to improve dissolution (Table 1). All mixtures resulted in clear and homogeneous solutions, and no precipitation was observed after cooling to room temperature, as previously reported for ChCl-based DESs using different acids (Craveiro et al. 2016; Fernandes et al. 2021). The acids and the molar ratios used to prepare the DESs are given in Table 1. Deep eutectic solvents (DESs) are chemical mixtures of two components or more, consisting of a hydrogen bond donor (HBD) and a hydrogen bond acceptor (HBA), in solid or liquid form, that are capable of combining via a hydrogen bond (Fig. 1). Images of the DESs are given in Figure S2 in Supplementary Information.

2.3 DES characterization

The viscosities of all DESs were measured using a HAAKE MARS III rheometer (Thermo Fisher Scientific) with cone/plate geometry (35 mm, 1 °, 0.052-mm gap) at different temperatures ranging from 25 to 150 °C. The densities of the four DES solutions were calculated by measuring the mass of a given volume.

2.4 DES pretreatment of wood

Each 150 × 75 × 15-mm wood sample was placed in a separate beaker containing 50 g DES and kept at 155 °C for 2 h. No mixing was applied during this process. At the end of the 2-h pretreatment period, the samples were washed with ethanol / water (15 mL, 1:1 molar ratio) to ensure that the DES was completely removed from the samples. This process was repeated three times and the samples were dried under vacuum. The control samples (untreated) were subjected to the same thermal stress, i.e., they were kept at 150 °C for 2 h.

2.5 Weathering test

To simulate outdoor conditions in the laboratory, the test and control samples were processed on the QUV accelerated weathering tester by applying UV-light for 8 h, followed by a water spray for 15 min (ASTM G154 2006). The average UV-light intensity in the test device was 340 nm and the temperature was adjusted to 45 °C. Four test and control groups were selected for each variation, and the wood surface changes in color, brightness, and roughness of the samples were examined and FTIR analyses were performed after 6, 12, 24, 48, 168, 336, 500, and 1000 h.

2.5.1 Color, gloss, roughness, and surface composition measurements

Prior to the weathering test, color measurements were performed on the control and test samples using the Konica Minolta CD-600 spectrophotometer. The color measurement analysis was carried out in accordance with the ISO 7724-1:1984 standard. Color measurements were taken from three different points (Fig. S3) on the prepared samples, and these were averaged. Four samples were used for each variation.

Gloss measurements of the wood surfaces were taken using the Konica Minolta gloss meter with a 60 ° measuring angle. The test device may be connected to a light source in parallel or in proximity to the light control test area, and the lens consists of a receiver containing a photocell receiver window. Gloss measurements were taken from three different points (Fig. S3 in Supplementary Information) on the prepared samples and averaged.

The surface quality measurements were performed using a MicroProf® FRT instrument (Fries Research & Technology GmbH, Bergisch Gladbach, Germany). The range of roughness parameters was calculated by the device, which included the arithmetic mean deviation of the assessed profile R_a. All the parameters were measured in 2D profile and three measurements were taken from the surface at each direction, i.e., one parallel-to-the-grain (number 1) and one perpendicular-to-the-grain (number 2), as shown in Figure S3. An evaluation length of 16 mm, a sampling length of 2.5 mm, and a measuring resolution of 5 µm were used with the scanning speed of 750 µm/s. A Gaussian filter was automatically applied to all roughness data.

Prior to the outdoor environment testing of the samples, chemical analyses were performed via a Shimadzu Fourier-transform infrared (FTIR) spectrometer. Using the Pike ATR Diamond/ZnSe accessory compatible with the Shimadzu model, solid measurements were taken from the surface without causing any damage to the samples. The spectra of the samples were obtained at a wavelength of 700–1800 cm^{-1} by performing 30 scans at a resolution of 4 cm^{-1}. The measured points were marked, and all testing periods were measured from the same points.

3 Results and discussion

3.1 Physicochemical properties of DES

The physicochemical properties of DES, i.e., density and viscosity, were tested, and the results are given in Table 1. The DES density values ranged from 1.21 to 1.31 g/cm^3, with those of the DESs prepared using betaine being higher.

The performance of DESs as extraction solvents largely depends on their ability to interact with the desired compound, and these interactions are affected not only by the chemical structure of the solvents, but also by their viscosity (Xu et al. 2020; Fernandes et al. 2021). Solvent viscosity has a direct effect on the mass transfer phenomenon, and therefore, high-viscosity solvents can hinder extraction efficiency (Dai et al. 2015). Some DESs have been reported to be highly viscous because of their strong hydrogen bonding networks that limit their ability to act as an extraction medium (Yang et al. 2015; Ghaedi et al. 2017). The temperature dependence of the viscosity of the DESs used in this study was evaluated at 25 and 150 °C, as reported in Table 1. As expected, the viscosity decreased slightly with the rise in temperature. At high temperatures, molecular bonds are formed and kinetic energy increases (Sarmad et al. 2017). At 25 °C, the betaine-based DESs were highly viscous, with viscosity values of 0.320 (AA-BT) and 0.895 Pa.s (OA-BT), compared to the ChCl-based DESs, with values ranging from 0.045 (AA-ChCl) to 0.120 Pa.s (OA-ChCl). Moreover, according to the results, the viscosity values of the acetic acid-based DESs were lower than those of the oxalic acid-based DESs. The carboxylic acid group present in acids can cause extra hydrogen bonding (Sarmad et al. 2017; El Achkar et al. 2019), which may have been responsible for the slightly superior viscosity values observed in the oxalic acid-based DESs. The viscosity values at the pretreatment temperature (i.e., 150 °C) exhibited more subtle differences compared to those at 25 °C.

3.2 Surface properties of DES-treated wood

The FTIR analysis of the test and control samples was carried out in the range of 1800 – 700 cm^{-1}. The assignments of the 14 characteristic peaks are listed in Table 2 (Colom et al. 2003; Dordevic et al. 2012; Cogulet et al. 2016; Fernandes et al. 2021). The FTIR analysis results of the samples treated with DESs are shown in Fig. 2.

Although it is hard to make comparisons with the signal of the C = O at 1728 cm^{-1}, a slight increase was seen for all modifications, which is logical by reason of the added C = O of the acids. According to the FTIR spectra of the controls and samples treated with DESs prepared with AA, the peak intensity increased for the 1728 cm^{-1} band, which belongs

Table 2 Characteristic IR absorption spectra bands in wood

Band	Wavenumber	Compound or chemical group
1	1728	C = O stretch of acetyl or carboxylic acid in hemicellulose
2	1610	Aromatic skeletal vibrations plus C = O stretch
3	1510 – 1504	Aromatic skeletal vibration in lignin
4	1470 – 1455	CH_2 of pyran ring symmetric scissoring; OH plane deformation vibration, antisymmetric and symmetric νCOO – vibrations
5	1365	C-H deformation in cellulose and hemicellulose
6	1315 – 1311	C-H vibration in cellulose
7	1265	C-O stretch lignin ring in guaiacyl units
8	1155	C-O-C asymmetric bridge in cellulose and hemicellulose
9	1100	Aromatic skeletal vibration and C-O stretch
10	1049	C-O vibration in cellulose and hemicellulose
11	1028	C-O vibration in cellulose and hemicellulose
12	950 – 930	-HC = CH- out of plane deformation (trans)
13	864	C-H deformation in cellulose
14	779	Cellulose

to the carbonyl and acetyl groups. However, a decrease was observed in the samples treated with DESs prepared with OA. The intensity of the other bands at the 1610 cm^{-1} region increased after DES pretreatment, except for AA-BT. The DES pretreatment of cellulose and hemicelluloses resulted in the formation of aldehyde and ketone groups on carbon atoms C2 and C3, which may have contributed to an increase in absorbance at the wavenumbers of 1610 cm^{-1}. It has also been reported that the formation of chromophoric carbonyl groups increases the intensity of the C = O band at 1630 cm^{-1} (Cogulet et al. 2016). This peak is also associated with the unbound C = C and water band. The intensity of absorption at 1615 cm^{-1} indicates paired α-C = O bonds with para-hydroxyphenyl groups. In this case, the water-absorbing H-O-H tension vibration in the carbohydrates was thought to increase after pretreatment. With the deformation of the H-O-H bond, the water absorption increased due to the increases in the hydroxyl group. Similar results have been found in many studies (Evans and Chowdhury 2010; Forsthuber et al. 2013; Saha et al. 2013). The 1510 – 1504 and 1265 cm^{-1} bands associated with lignin decreased after DES pretreatment.

The peak of the aromatic cellulose rings at 1470 – 1455 cm^{-1} shows C = C and CH_2 vibrations. This peak also shows the change in the crystalline and amorphous structure of the cellulose. Compared to the amorphous region, the crystalline region of the cellulose increased after the pretreatment with ChCl-based DESs. Other bands at 1365, 1315 – 1311, 1155, 1100, 1049, 1028, 950 – 930, 864, and 779 cm^{-1} are mainly associated with carbohydrates. These bands increased significantly after DES treatment, especially at 1470 – 1455, 1315 – 1311, and 950 – 930 cm^{-1}. The increase in these bands was due to the structure of AA and OA. When the spectra of the control wood and the DES-treated samples were compared, supplementary bands were

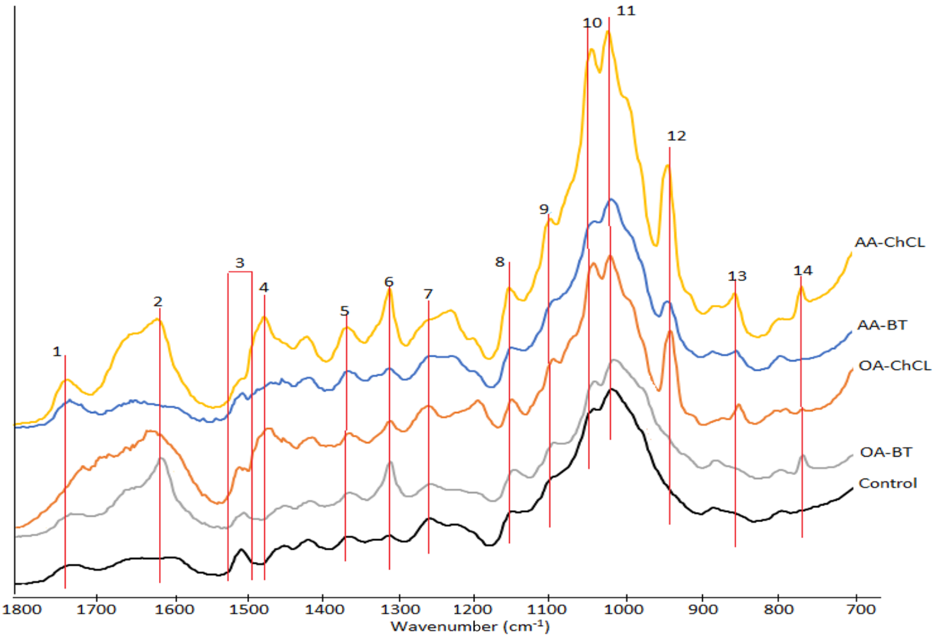

Fig. 2 FTIR-ATR spectra of Scots pine (control) and DES-treated wood

noted in the DES-treated wood. This could be attributed to the nature of the chemical interaction between the studied DESs and the wood.

Table 3 indicates the color changes (ΔL*, Δa*, Δb*, ΔE*), gloss (60 °) and surface roughness (Ra) values along with the SD. The values in Table 3 were measured on the wood surfaces after DES pretreatment. The points where the measurements were taken are shown in Fig. 2.

Negative and positive values showed a tendency of the wood surface to become greenish and reddish for Δa*, and bluish and yellowish for Δb*, respectively (Hunter 2008). Except for the OA-ChCl pretreatment, the other DES pretreatments caused the surfaces to redden and become yellowish. The negative lightness stability (ΔL*) indicated a tendency of the wood surface to become darker, with maximum darkening observed on the OA-ChCl-treated wood surface. Color change is also correlated to carbonyl formation as well as lignin degradation (Pandey 2005). The FTIR peaks at 1504 cm^{-1} (lignin degradation) and 1728 cm^{-1} (carbonyl group formation) were linearly correlated with ΔE* in studies by Müller et al. (2003) and Yildiz et al. (2013).

The brightness values of the DESs-treated Scots pine wood samples were seen to increase in the AA-treated samples, whereas they decreased in the OA-modified samples. With lignin degradation, the rising cellulose ratio on the wood surfaces increased the brightness of the samples. The lowest brightness value (2.0) was obtained in samples modified with OA-ChCl. When the total color change was examined, the highest color change was observed in this group (OA-ChCl). Photographic images of the DES-treated wood are presented in Figure S4 in Supplementary Information, which show that high erosion (Ra of 8.68) occurred on the surfaces of the samples after DES pretreatment. Thus, the wood fibers were separated from the wood surface and the light applied during the brightness measurement was refracted and reflected, causing the brightness value to decrease.

The surface roughness (Ra) values of the DES-treated samples are given in Table 3. After DES pretreatment, the parallel-to-the-grain roughness of all samples increased. However, this increase was not significant for DES solutions prepared with ChCl, whereas significant increases were observed for solutions prepared with BT. This was likely due to changes of surface composition caused by micro cracks after DES pretreatment with BT. Another reason for rougher surfaces could have been that with DES, some wood surface components, primarily hemicelluloses and lignin, were leached from solvent controls.

3.3 Surface properties of weathered wood

Weathering initiates a wide variety of chemical changes in the wood surface. With the weathering process, lignin and hemicellulose, which are the main components of wood, are significantly affected. The change in wood components caused by weathering was determined by ATR-FTIR analysis. Figure 3 shows the Scots pine (control) and Figs. 4, 5, 6 and 7 the DES-treated test samples. The carbonyl and acetyl groups in hemicellulose at the 1730 cm^{-1} peak decreased in all variations. This peak disappeared after 500 h. This can be explained by the degradation of the acetyl groups and leaching of the degraded carbonyl groups from the water during accelerated weathering (Arpaci et al. 2021). Another band, 1615 cm^{-1}, which emerged after the DES pretreatment process, increased significantly in the OA-treated samples in parallel with the increase in the weathering time, whereas the band decreased in the AA-treated samples. The formation of chromophoric carbonyl groups caused the C = O band to increase.

The most sensitive wood constituent is lignin, which can be studied via a reference peak at 1504–1510 cm^{-1} (lignin band). The lignin peak decreased over time in the control samples. After 500 h of weathering, it had completely disappeared. Ultra-violet radiation leads to lignin decomposition (photolysis) and consequently, to delamination of surface fibers. In particular, the chromophoric groups of lignin are strong UV absorbers that are responsible for yellowing of the surface. The most pronounced reduction in intensity was evident for band 1510 cm^{-1} and is related to the degradation of lignin caused by UV radiation. Other researchers have reported similar findings for laboratory experiments after observing a decrease in peaks assigned to lignin over the irradiation time span (Timar et al. 2016; Sandak et al. 2021). Lignin and extractives are considered to be absorbers of UV radiation; therefore, these components suffered major degradation (Timar et al. 2016; Sandak et al. 2021). A reduction was also observed in the DES-treated variations. The minimum decrease was in the AA-BT samples.

Table 3 Color changes, gloss, and surface roughness values of control and DES-treated samples

	Color changes				Gloss (60°)	Surface roughness (Ra)
	ΔL*	Δa*	Δb*	ΔE*		
Control	-	-	-	-	2.7 (0.04)	7.12 (0.40)
AA-ChCl	-17.56 (1.23)	5.51 (0.55)	3.09 (0.09)	18.74 (0.90)	3.0 (0.10)	7.82 (1.39)
AA-BT	-15.98 (1.45)	5.61 (0.43)	2.48 (0.34)	17.19 (2.31)	2.9 (0.94)	10.05 (1.45)
OA-ChCl	-41.19 (3.98)	0.86 (0.02)	-12.16 (1.11)	43.11 (3.45)	2.0 (0.06)	8.68 (1.07)
OA-BT	-11.79 (0.79)	4.32 (0.97)	1.75 (0.07)	12.72 (1.27)	2.2 (0.50)	10.63 (1.10)

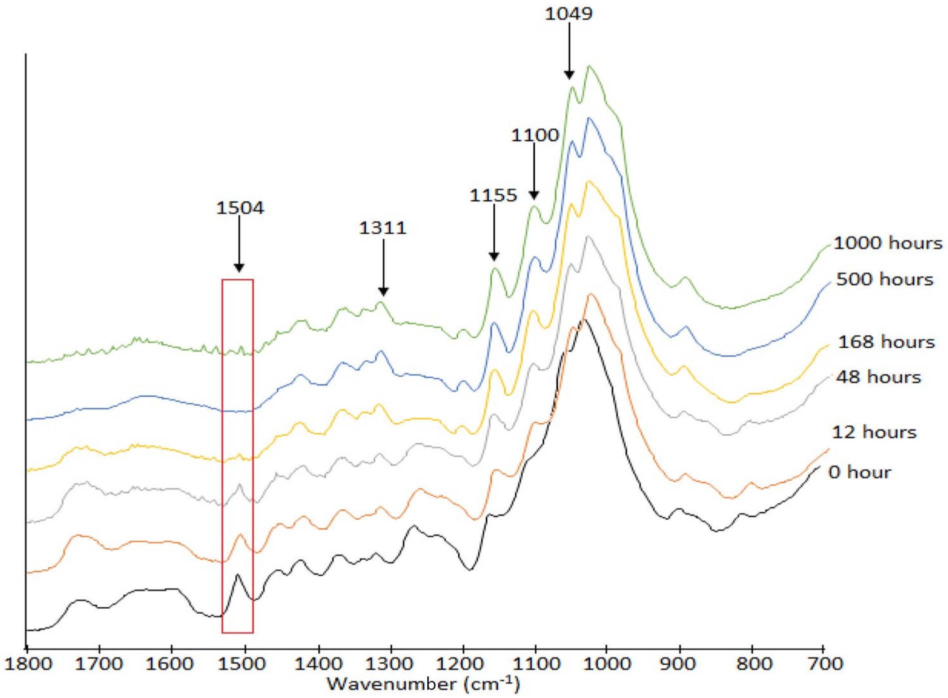

Fig. 3 FTIR-ATR spectra of Scots pine wood (control) corresponding to different exposure periods of 0–1000 h

The peak at 1315 – 1313 cm^{-1} was attributed to the CH_2 functional group of cellulose crystallinities (Colom and Carrillo 2002). This peak increased significantly after DES pretreatment. Peak values continued to increase after weathering. The increase was limited in the control and samples treated with DES solutions prepared with AA. However, significant increases were observed in samples treated with DES solutions prepared with OA. This result was due to the reduction in the amorphous zones of the cellulose, which led to the increase in the crystal content (Can et al. 2019).

Carbohydrate peaks, such as 1155, 1100, 1049 – 1026 cm^{-1}, which are mostly found in cellulose, increased in all variations. The intensity of the 950 – 930 cm^{-1} region increased after DES pretreatment. The intensity of this band decreased with the weathering. Moreover, this band decreased after 168 h for the OA-ChCl-treated samples. For the samples modified with OA-ChCl and OA-BT, the peak related to cellulose at about 779 – 715 cm^{-1} significantly increased with the longer weathering exposure.

A semi-quantitative method was used to analyze the hemicellulose/cellulose intensity ratio (I1730/I1154), C = O stretching conjugated to the aromatic ring (I1615), degradation of lignin (I1504/I1365), lignin/cellulose intensity ratio (I1504/I1154), and crystallinity index (I1313/I1335) during weathering, as shown in Table 4. The hemicellulose/cellulose intensity ratio (I1730/I1154) declined with increasing weathering duration. The intensity increased slightly in the first 48 h for the control and OA-BT-modified wood, and in the first 12 h, for samples modified with AA-ChCl and AA-BT. The creation of aldehyde and ketone groups has been reported to be the cause (Arpaci et al. 2021). The C = O stretching conjugated to the aromatic ring (I1615) was increased. The carbonyl contribution rose from 0.035 to 0.042 after 168 h for the control. After 12 h of weathering time, this ratio decreased for the control samples, whereas increases were observed in those treated with the DES solution variations. This new carbonyl structure was associated with the new color. The color results supported this situation (Fig. 8). Table 4 indicated the ratio I1504/I1365 as a function of weathering time. This parameter decreased from 0.780 to 0.455 for the control samples. This value decreased in parallel with the increase in weathering time in the DES-modified samples. A reduction of 115.74% was observed in the samples exposed to AA-ChCl and 66.33% in the samples exposed to AA-BT (Table 4). Similar results for pine and spruce were reported in the literature (Pandey 2005; Cogulet et al. 2016)

The lignin/cellulose intensity ratio (I1504/I1154) value significantly decreased for the AA-ChCl and AA-BT modified wood. This value showed a decrease in all variations with increased weathering time. Although a 57% reduction was observed in the control samples after 500 h, a 67.97% reduction was obtained in the AA-ChCl-modified samples. This situation proved that lignin degradation had not been completed after 1000 h of accelerated weathering. These reductions in all variations demonstrated that the lignin on

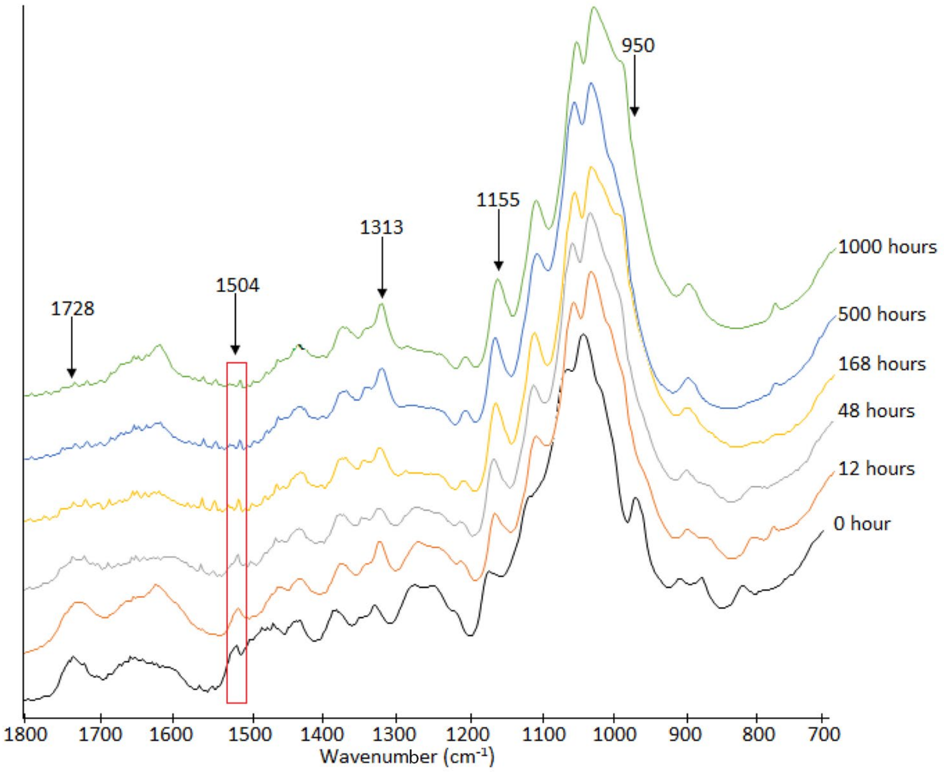

Fig. 4 FTIR-ATR spectra of AA-BT treated wood corresponding to different exposure periods of 0–1000 h

the wood surfaces was significantly reduced by the weathering process. An increase in the I1318/I1335 ratio implied an increase in crystallinity (Table 4). The crystallinity index increased from 1.069 to 1.105 for the control and from 1.135 to 2.237 for the OA-ChCl samples. Similarly, an increase of 78.39% was observed in the OA-BT-modified samples (Table 4). This finding is compatible with the literature (Colom et al. 2003; Müller et al. 2003). The increased crystallinity declined in some cases. Cellulose, even when crystallized, can be depolymerized under long weathering time

The macroscopic evaluation after weathering of the wood is shown in Figure S4. The Scots pine, whose natural color is yellow, had turned brown with the weathering time. The color turned gray after 500 h of weathering. This change was more pronounced in the test samples.

The color changes (ΔL*, Δa*, Δb*, and ΔE*) in the weathered samples for parallel-to-the-grain (∥) are shown in Fig. 8, gloss changes in Fig. 9, and surface roughness (Ra) in Fig. 10.

A negative lightness stability (ΔL*) indicates the tendency of a wood surface to become darker. The ΔL* decreased from −5.70 to -17.21 and then increased to -13.05 for the control samples. It was a different case for the test samples. Although a negative ΔL* was observed in the initial period of the weathering process, after 48 h, a significant increase was seen for the AA-based DES samples. The ΔL* values of the test samples tended to decrease up to 168–336 h of weathering for the OA-based DES-treated wood, but afterwards, they tended to increase. The degradation of lignin dominated the surface color change process at first, resulting in the whitening of the wood samples. The darkening of the wood with increasing time might have been due to existences of micro cracks and the migration of surface wood components. After that, with increasing time, the extractives volatilized or degraded. Therefore, the wood surface became white again. In the last stage of weathering, the ΔL* values were influenced by the complex process of lignin and extractive degradations, which can lead to the instability of ΔL* values (Arpaci et al. 2021).

The redness/greenness values for the weathered samples are shown in Fig. 8. The redness index (+Δa*) of the control and test samples showed an increasing trend up to 168 h of weathering, but then began to decrease significantly, evidently in parallel with the increase in the weathering period. At the end of the test, all test samples showed a greenness index, and the control samples showed a redness index. The Δa* increased from 0.34 to 5.76 after 168 h of weathering time. Except for the OA-ChCl-treated wood, the yellowness index (+Δb*) of the control and test samples exhibited

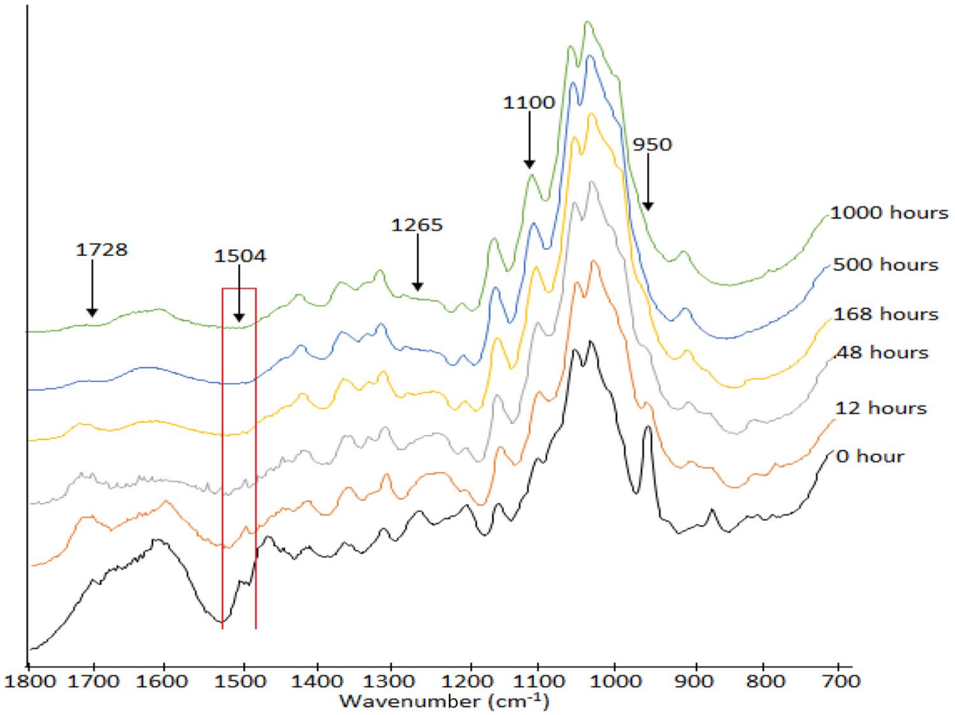

Fig. 5 FTIR-ATR spectra of AA-ChCl treated wood corresponding to different exposure periods of 0–1000 h

an increasing trend during the 48 h of weathering. However, thereafter, it began to decrease significantly, evidently in parallel with the increase in the weathering period. At the end of the test, all test samples exhibited a blueness index (-Δb*). Photo-yellowing was correlated very well with lignin degradation. The absorption between 1600 and 1690 cm^{-1} showed the formation of conjugated carbonyl bands in the quinone range, which is associated with the decay of aromatic structures and the formation of conjugated carbonyl groups (Arpaci et al. 2021).

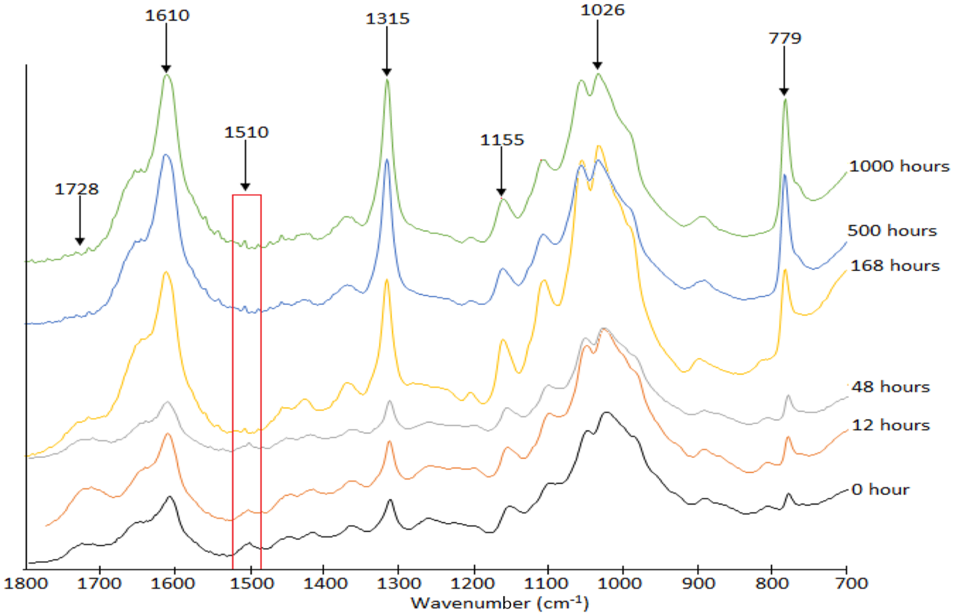

Fig. 6 FTIR-ATR spectra of OA-BT treated wood corresponding to different exposure periods of 0–1000 h

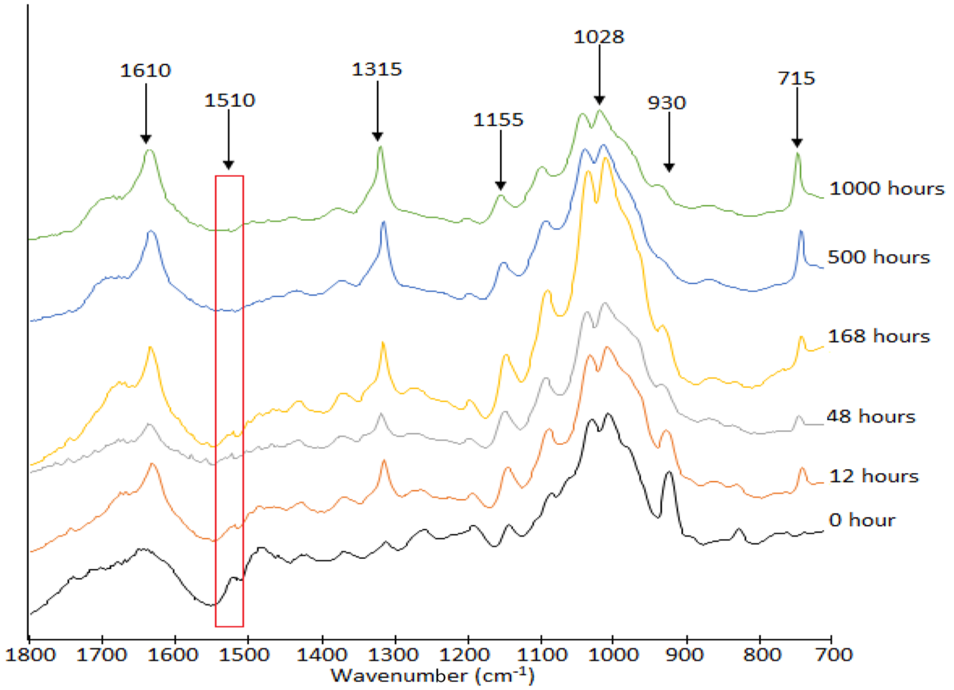

Fig. 7 FTIR-ATR spectra of OA-ChCl treated wood corresponding to different exposure periods of 0–1000 h

The total color change (ΔE*) gradually increased in parallel with the weathering period up to 168 h of weathering time. In general, the color change of the samples was found to be greater during the initial period of accelerated weathering, probably as a result of the instigation of lignin photo-degradation, and afterwards, the color continued to change, but at a slower rate. In addition, according to the FTIR results, it seems that the lignin peaks disappeared after 48–168 h of weathering. The decrease or disappearance of lignin peak values in the wood samples indicated the reason that the color change had remained stable or decreased. These DESs can be easily recycled and reused several times without compromising extraction performance or originality. A number of literature studies have been published on this subject (Li et al. 2018; Tang and Row 2020; Wang et al. 2020).

Wood gloss change was not affected as much by weathering conditions as were changes in color and roughness. In the study, the gloss change of the control samples increased in parallel with the increase in weathering time. Similar results were also found in the case of samples treated with DESs prepared with AA. However, in the samples treated with DESs prepared with OA, the gloss changes decreased after 48 h for BT and after 168 h for ChCl. In the accelerated weathering test, the minimum gloss change was obtained in the OA-BT treated samples and the maximum gloss change in the AA-ChCl treated samples. It was observed that the gloss values of the wood samples treated with OA-BT and OA-ChCl remained stable after 168 h of weathering.

Changes in brightness and color occur as a result of exposure of wood to external weather conditions for a short time. In some wood species such as redwood, Scots pine, and fir, the brightness significantly decreases in the first months. However, it was observed that the brightness values of samples that remained in outdoor weather conditions for a period of six months had increased again. When western red cedar specimens were exposed to external weather conditions, their brightness values increased in the first six months, but decreased in the following months (Feist 1990a). Several studies have reported that as a result of the exposure of wood samples to water and UV rays, the brightness values decreased in the initial time periods and then increased with increased passing of time. A possible explanation for this is that in the early stages of the photodegradation process, the dark surfaces formed by the breakdown of lignin reduces the brightness values, and with the progress of time, these lignin components become separated from the wood by the effect of water. The decrease in the ratio of lignin on the wood surface causes the cellulose content to increase. Cellulose, which has a white, bright structure, increases the brightness values of wood surfaces (Hon and Feist 1986; Feist 1990b; Ormondroyd et al. 2015). In their study, Hon and Feist (1986) exposed white oak, red oak, poplar, and sweetgum wood to accelerated outdoor tests and natural outdoor tests. Regardless of the exposure conditions, the

Table 4 Hemicellulose/cellulose intensity (I1730/I1154), C = O stretching aromatic ring (I1615), degradation of lignin (I1504/I1365), lignin/cellulose intensity ratio (I1504/I1155), and crystallinity index (I1313/I1335) of the weathered samples

	Test time (h)	I1730/I1154	I1615	I1504/I1365	I1504/I1155	I1313/ I1335
Control	0	0.388	0.035	0.780	0.551	1.069
	12	0.487	0.042	0.695	0.469	1.101
	48	0.511	0.022	0.725	0.503	1.083
	168	0.362	0.037	0.456	0.306	1.099
	500	0.258	0.034	0.359	0.235	1.125
	1000	0.258	0.031	0.455	0.289	1.105
OA-ChCl treated	0	0.457	0.099	0.697	0.535	1.135
	12	0.358	0.125	0.618	0.448	1.420
	48	0.377	0.082	0.710	0.501	1.325
	168	0.300	0.159	0.582	0.418	1.444
	500	0.271	0.111	0.458	0.347	1.947
	1000	0.286	0.103	0.479	0.374	2.237
OA-BT treated	0	0.463	0.085	0.662	0.479	1.546
	12	0.599	0.123	0.583	0.398	1.540
	48	0.523	0.074	0.688	0.465	1.618
	168	0.413	0.217	0.513	0.363	1.964
	500	0.320	0.192	0.581	0.453	2.922
	1000	0.303	0.211	0.582	0.462	2.758
AA-ChCl treated	0	0.455	0.100	0.699	0.533	1.155
	12	0.513	0.062	0.602	0.435	1.196
	48	0.426	0.036	0.555	0.394	1.109
	168	0.284	0.042	0.322	0.212	1.131
	500	0.188	0.054	0.285	0.176	1.142
	1000	0.222	0.035	0.324	0.198	1.188
AA-BT treated	0	0.405	0.031	0.672	0.484	1.107
	12	0.466	0.062	0.602	0.411	1.185
	48	0.392	0.028	0.636	0.412	1.102
	168	0.344	0.025	0.567	0.355	1.122
	500	0.225	0.032	0.404	0.252	1.213
	1000	0.242	0.066	0.404	0.263	1.246

color and brightness values of all wood samples decreased. As a result of the photodegradation of the wood, the chromophoric structures in the emerging lignin absorbed light. During the brightness measurement, the light falling on the sample surface was absorbed by the lignin and caused the measured value to be low.

Change in roughness was characterized in terms of average surface roughness (Ra), as presented in Fig. 10. The wood surface became rougher after 1000 h of accelerated weathering. The roughness increased in parallel with the accelerated weathering time for the control samples. After 1000 h of weathering, the roughness values of the control samples increased by 88.88% compared to their initial values. The samples modified with OA-ChCl showed a reduction in roughness up to 48 h, and all other test samples up to 500 h, i.e., the roughness values of the samples treated with DESs decreased up to 500 h weathering except for the OA-ChCl samples. Significant increases were observed in the roughness values of the test samples after 500 h of weathering. The roughness value decreased by -35.35% for AA-ChCl, -29.63% for AA-BT, and − 15.16% for OA-BT after 500 h of weathering; however, this value increased by 34.78%, 26.74%, and 19.73% after 1000 h, respectively. The increase in wood surface roughness was attributed to the degradation of wood polymers (especially lignin) and the removal of degraded compounds from the wood via the leaching with water (Feist 1982; Behbood and Saei 2015). This finding was also supported by the FTIR analysis results. In previous studies, it was stated that the roughness values of samples had increased with the weathering process (Nzokou et al. 2011; Behbood and Saei 2015). The highest mean value of Ra* after weathering was observed for the control (Ra = 15.50 µm), whereas the lowest was for the AA-ChCl-treated wood (Ra = 9.19 µm). The most interesting finding from this study was that the roughness values of the test samples decreased with weathering up to 500 h. The varied behavior of the control and test samples for the first 500 h of the weathering period resulted from the different chemical structures of the samples. Examination of the FTIR results showed that the chemical structure of the test

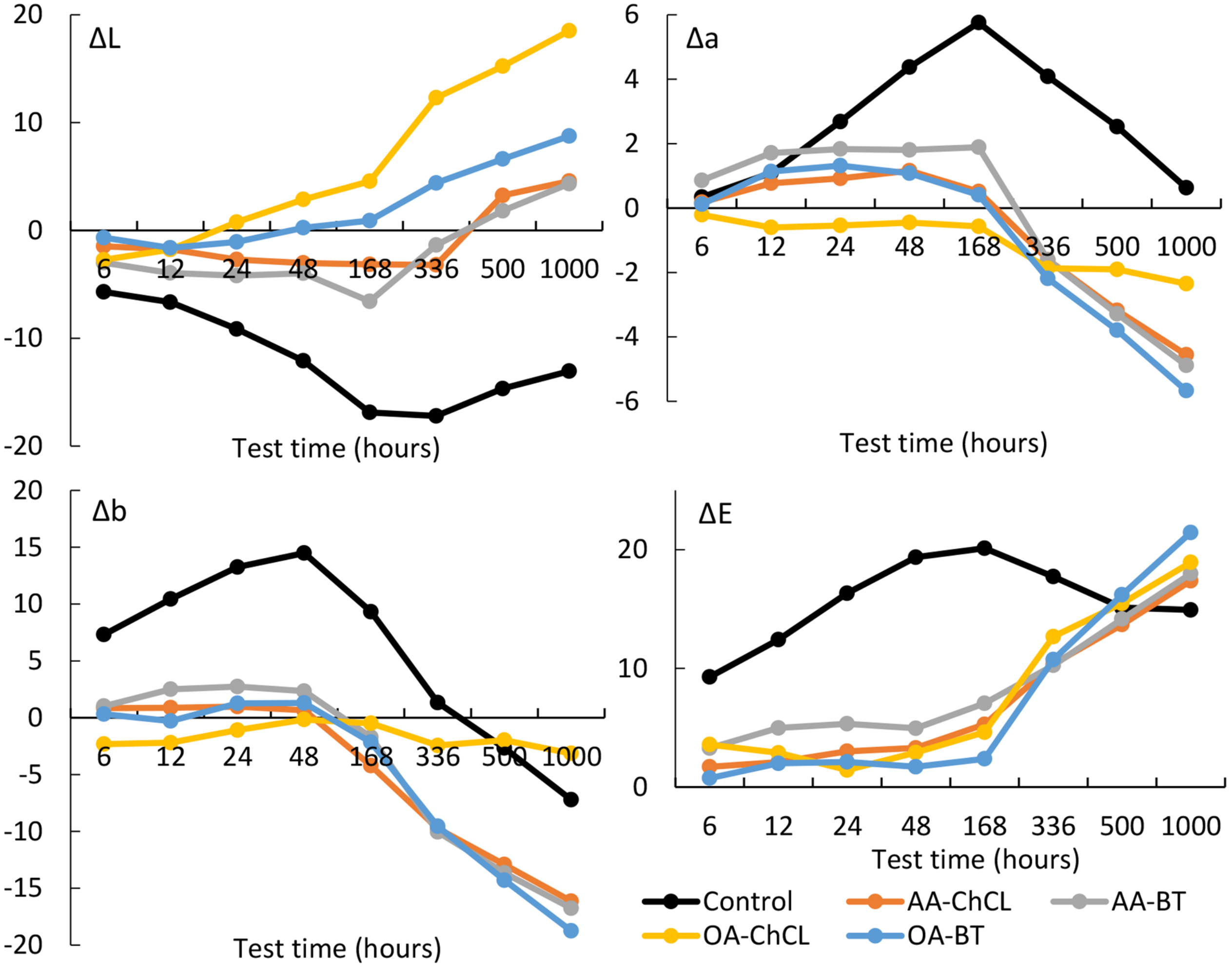

Fig. 8 Color changes due to accelerated weathering. Variation of CIELAB parameters ΔL*, Δa*, Δb*, and ΔE* on the surface of Scots pine wood at different accelerated weathering times

samples treated with DESs differed from those of the control samples. New peak (1615, 1313, 1100, 950 cm^{-1}) values were formed in the wood samples after DES pretreatment. Control and test samples having different chemical structures were expected to exhibit different behaviors against weathering. In the literature studies, it has been stated that the roughness behavior in wood species differs depending on the different chemical contents (Temiz 2005; Tolvaj et al. 2014; Tomak et al. 2018).

4 Conclusion

Several acidic DESs were prepared and characterized for their physicochemical properties. Scots pine wood samples were treated on the surface with acidic DESs that included acetic acid-choline chloride (AA-ChCl), acetic acid-betaine (AA-BT), oxalic acid-choline chloride (OA-ChCl), and oxalic acid-betaine (OA-BT). The experimental results for the physicochemical parameters showed that the four DESs had low density and good viscosity. The Scots pine wood samples were treated with the DES solutions at 150 °C. According to the FTIR results, chemical changes at 1504 cm^{-1} (lignin degradation) and 1728 cm^{-1} (carbonyl group formation) on the DES-treated sample surfaces led to color changes in the wood. The color maintenance of wood treated with the DESs after accelerated weathering for 168 h demonstrated the potential of the tested DESs as useful "green" alternatives to traditional toxic UV stabilizers. Considering the favorable "green" features of this new solvent treatment and its remarkable extraction capacity and selectivity for lignin (even after recycling), this process could prove to be highly attractive for future large-scale applications.

Authorship contribution statement.

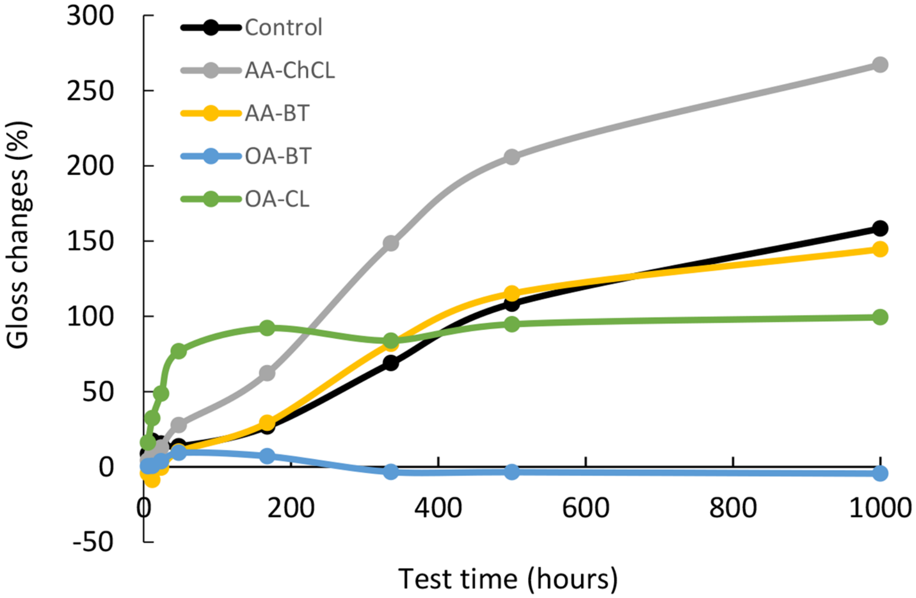

Fig. 9 Gloss changes of weathered samples at different accelerated weathering times

Ahmet E. Çelik: Conceptualization, Methodology, Investigation, Data curation, Visualization, Writing - original draft.

Ahmet Can: Funding acquisition, Project administration, Conceptualization, Methodology, Data curation, Writing - review & editing.

Supplementary information The online version contains supplementary material available at https://doi.org/10.1007/s00107-022-01843-1.

Funding This study was funded by the Turkish Scientific and Research Council (TUBITAK) under Project number 2209-1919B011902663. Ahmet Emre Çelik is an undergraduate student and served as the project coordinator.

Declarations

Conflict ing Interest.

We wish to declare that there are no known conflicts of interest associated with this publication and there has been no significant financial sup-

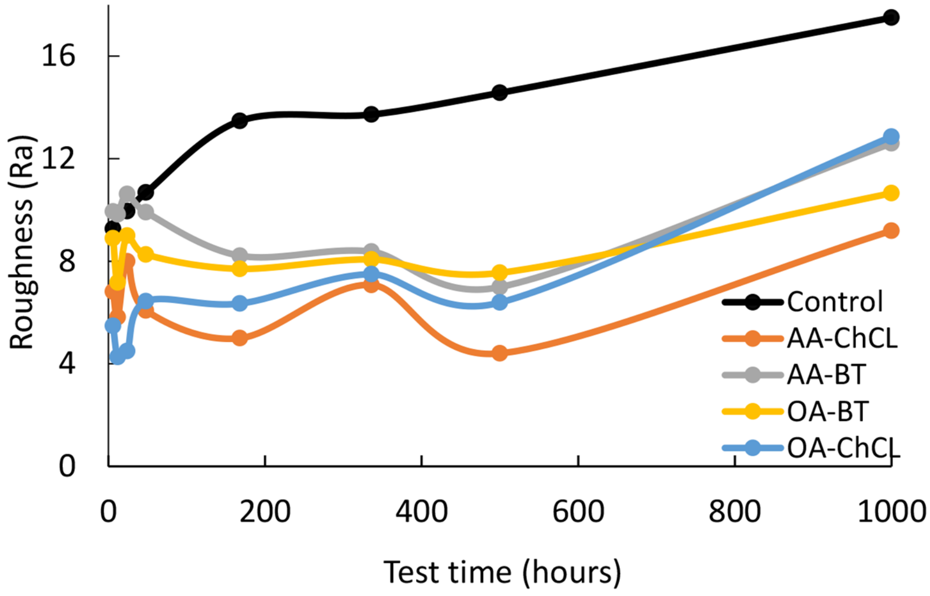

Fig. 10 Roughness (Ra) of weathered samples

port for this work that could have influenced its outcome.

Supplementary materials.

Supplementary materials associated with this article can be found in the online version at DOI:

References

Abbott AP, Capper G, Davies DL, Rasheed RK, Tambyrajah V(2003) Novel solvent properties of choline chloride/urea mixtures. Chemical communications 1:70–71

Alvarez-Vasco C, Ma R, Quintero M, Guo M, Geleynse S, Ramasamy KK, Wolcott M, Zhang X (2016) Unique low-molecular-weight lignin with high purity extracted from wood by deep eutectic solvents (DES): a source of lignin for valorization. Green Chem 18(19):5133–5141

Arpaci SS, Tomak ED, Ermeydan MA, Yildirim I (2021) Natural weathering of sixteen wood species: Changes on surface properties. Polym Degrad Stab 183:109415

ASTM G154-06 (2006) Standard practice for operating fluorescent light apparatus for UV exposure of nonmetallic materials ASTM International, West Conshohocken, PA, USA

Behbood M, Saei AM (2015) Effects of geographical directions and climatological parameters on natural weathering of fir wood Constr. Build Mater 94:684–690

Boerjan W, Ralph J, Baucher M (2003) Lignin biosynthesis. Annu Rev Plant Biol 54(1):519–546

Can A, Palanti S, Sivrikaya H, Hazer B, Stefanı F (2019) Physical, biological and chemical characterisation of wood treated with silver nanoparticles. Cellulose 26(8):5075–5084

Cogulet A, Blanchet P, Landry V (2016) Wood degradation under UV irradiation: A lignin characterization. J Photochem Photobiol B 158:184–191

Colom X, Carrillo F (2002) Crystallinity changes in lyocell and viscose-type fibres by caustic treatment. Eur Polymer J 38(11):2225–2230

Colom X, Carrillo F, Nogués F, Garriga P (2003) Structural analysis of photodegraded wood by means of FTIR spectroscopy. Polym Degrad Stab 80(3):543–549

Cox P, Wilkinson SP, Anderson JM (2001) Effects of fungal inocula on the decomposition of lignin and structural polysaccharides in Pinus sylvestris litter. Biol Fertil Soils 33(3):246–251

Craveiro R, Aroso I, Flammia V, Carvalho T, Viciosa MT, Dionísio M, Barreiros S, Reis RL, Duarte ARC, Paiva A (2016) Properties and thermal behavior of natural deep eutectic solvents. J Mol Liq 215:534–540

Dai Y, Witkamp GJ, Verpoorte R, Choi YH (2015) Tailoring properties of natural deep eutectic solvents with water to facilitate their applications. Food Chem 187:14–19. https://doi.org/10.1016/j.foodchem.2015.03.123

Dordevic DM, Stankovic MN, Dordevic MG, Krstić NS, Pavlović MA, Radivojević AR, Filipović IM (2012) FTIR spectroscopic characterization of bituminous limestone: Maganik mountain (Montenegro), vol 57. Studia Universitatis Babes-Bolyai, Chemia, 4

El Achkar T, Fourmentin S, Greige-Gerges H (2019) Deep eutectic solvents: An overview on their interactions with water and biochemical compounds. J Mol Liq 288:111028. https://doi.org/10.1016/j.molliq.2019.111028

Evans PD, Chowdhury MJ (2010) Photoprotection of wood using polyester-type UV-absorbers derived from the reaction of 2-hydroxy-4 (2, 3-epoxypropoxy)-benzophenone with dicarboxylic acid anhydrides. J Wood Chem Technol 30(2):186–204

Faruk O, Sain M (2015) Lignin in polymer composites. William Andrew. William Andrew Publishing, pp 1–11

Feist WC(1982) Weathering of wood in structural uses R.W. Meyer, R.M. Kellogg (Eds.), Structural Use of Wood in Adverse Environments, Van Ostrand Reinhold (1982), pp. 156–207

Feist WC (1990a) Outdoor wood weathering and protection. Archaeological wood, properties, chemistry, and preservation. Adv Chem Ser 225:263–298

Feist WC (1990b) Weathering performance of painted wood pretreated with water-repellent preservatives. For Prod J 40(7/8):21–26

Fengel D, Wegener G(2011) Wood: Chemistry, Ultrastructure, Reactions Walter de Gruyter, pp. 1-626, https://doi.org/10.1007/BF02608943

Fernandes C, Melro E, Magalhães S, Alves L, Craveiro R, Filipe A, Romano A, Medronho B (2021) New deep eutectic solvent assisted extraction of highly pure lignin from maritime pine sawdust (*Pinus pinaster* Ait.). Int J Biol Macromol 177:294–305

Forsthuber B, Müller U, Teischinger A, Grüll G (2013) Chemical and mechanical changes during photooxidation of an acrylic clear wood coat and its prevention using UV absorber and micronized TiO2. Polym Degrad Stab 98(7):1329–1338

Francisco M, van den Bruinhorst A, Kroon MC (2012) New natural and renewable low transition temperature mixtures (LTTMs): screening as solvents for lignocellulosic biomass processing. Green Chem 14(8):2153–2157

Ghaedi H, Ayoub M, Sufian S, Shariff AM, Lal B (2017) The study on temperature dependence of viscosity and surface tension of several Phosphonium-based deep eutectic solvents. J Mol Liq 241:500–510

Gunny AAN, Arbain D, Nashef EM, Jamal P (2015) Applicability evaluation of Deep Eutectic Solvents–Cellulase system for lignocellulose hydrolysis. Bioresour Technol 181:297–302

Holmbom B, Ekman R, Eckerman C (1992) Degradation products formed during light and heat treatment of spruce groundwood. J Pulp Pap Sci 18(4):J146–J151

Hon DNS, Shiraishi N(2001) Wood and Cellulosic Chemistry (second ed.), CRC Press, New York (2001)

Hon DS, Feist WC (1986) Weathering characteristics of hardwood surfaces. Wood Sci Technol 20(2):169–183

Hunter (2008) Associates Laboratory CIEL*a*b* color scale Applications note-insight on color HenterLab, 8 (9), pp. 1–4

ISO 7724- 1:1984 Paints and varnishes - Colorimetry- Part 1: Principles.International Organization for Standardization, Geneva, Switzerland

Kim KH, Dutta T, Sun J, Simmons B, Singh S (2018) Biomass pretreatment using deep eutectic solvents from lignin derived phenols. Green Chem 20(4):809–815

Li WX, Xiao WZ, Yang YQ, Wang Q, Chen X, Xiao LP, Sun RC (2021) Insights into bamboo delignification with acidic deep eutectic solvents pretreatment for enhanced lignin fractionation and valorization. Ind Crops Prod 170:113692

Li P, Sirviö JA, Asante B, Liimatainen H (2018) Recyclable deep eutectic solvent for the production of cationic nanocelluloses. Carbohydr Polym 199:219–227

Liu QP, Hou XD, Li N, Zong MH (2012) Ionic liquids from renewable biomaterials: synthesis, characterization and application in the pretreatment of biomass. Green Chem 14(2):304–307

Liu Y, Chen W, Xia Q, Guo B, Wang Q, Liu S, Yu H (2017) Efficient cleavage of lignin–carbohydrate complexes and ultrafast extraction of lignin oligomers from wood biomass by microwave-assisted treatment with deep eutectic solvent. Chemsuschem 10(8):1692

Lynam JG, Kumar N, Wong MJ (2017) Deep eutectic solvents' ability to solubilize lignin, cellulose, and hemicellulose; thermal stability; and density. Bioresour Technol 238:684–689

Mahmood Z, Yameen M, Jahangeer M, Riaz M, Ghaffar A, Javid I(2018) Lignin as Natural Antioxidant Capacity. In Lignin-Trends and Applications; IntechOpen: London, UK, pp. 181–205

Malaeke H, Housaindokht MR, Monhemi H, Izadyar M (2018) Deep eutectic solvent as an efficient molecular liquid for lignin solubilization and wood delignification. J Mol Liq 263:193–199

Morais ES, Freire MG, Freire CS, Coutinho JA, Silvestre AJ (2020) Enhanced conversion of xylan into furfural using acidic deep eutectic solvents with dual solvent and catalyst behavior. Chemsuschem 13(4):784–790

Müller U, Rätzsch M, Schwanninger M, Steiner M, Zöbl H (2003) Yellowing and IR-changes of spruce wood as result of UV-irradiation. J Photochem Photobiol B 69(2):97–105

Nzokou P, Kamdem DP, Temiz A (2011) Effect of accelerated weathering on discoloration and roughness of finished ash wood surfaces in comparison with red oak and hard maple. Prog Org Coat 71(4):350–354. https://doi.org/10.1016/j.porgcoat.2011.03.028

Ormondroyd G, Spear M, Curling S(2015) Modified wood: review of efficacy and service life testing. Proceedings of the Institution of Civil Engineers-Construction Materials, 168(4), 187–203

Pandey KK (2005) A note on the influence of extractives on the photo-discoloration and photo-degradation of wood. Polym Degrad Stab 87(2):375–379

Perez-Sanchez M, Sandoval M, Hernaiz MJ, Maria PDD (2013) Biocatalysis in biomass-derived solvents: the quest for fully sustainable chemical processes. Curr Org Chem 17(11):1188–1199

Rowell R, Pettersen R, Han J, Rowell J, Tshabalala MA(2005) Cell wall chemistry. Handbook of wood chemistry and wood composites. Taylor & Francis Group. Ed., 1, 70–71

Saha S, Kocaefe D, Boluk Y, Pichette A (2013) Surface degradation of CeO2 stabilized acrylic polyurethane coated thermally treated jack pine during accelerated weathering. Appl Surf Sci 276:86–94

Sandak A, Sandak J, Noël M, Dimitriou A (2021) A method for accelerated natural weathering of wood subsurface and its multilevel characterization. Coatings 11(2):126. https://doi.org/10.3390/coatings11020126

Sarmad S, Xie Y, Mikkola JP, Ji X (2017) Screening of deep eutectic solvents (DESs) as green CO 2 sorbents: from solubility to viscosity. New J Chem 41(1):290–301. https://doi.org/10.1039/c6nj03140d

Sinclair A, Jiang L, Bajwa D, Bajwa S, Tangpong S, Wang X (2018) Cellulose nanofibers produced from various agricultural residues and their reinforcement effects in polymer nanocomposites. J Appl Polym Sci 135(21):46304

Smolarski N (2012) High-value opportunities for lignin: unlocking its potential. Frost & Sullivan 1:1–15

Tang W, Row KH (2020) Design and evaluation of polarity controlled and recyclable deep eutectic solvent based biphasic system for the polarity driven extraction and separation of compounds. J Clean Prod 268:122306

Temiz A(2005) The effect of simulated weathering on preservative treated wood Doctoral dissertation, Thesis of PhD, KTÜ, Institute of Science and Technology, Trabzon, 2005

Tian D, Chandra RP, Lee JS, Lu C, Saddler JN (2017) A comparison of various lignin-extraction methods to enhance the accessibility and ease of enzymatic hydrolysis of the cellulosic component of steam-pretreated poplar. Biotechnol Biofuels 10(1):1–10

Timar MC, Varodi AM, Gurău L (2016) Comparative study of photodegradation of six wood species after short-time UV exposure. Wood Sci Technol 50(1):135–163

Tolvaj L, Molnar Z, Magoss E (2014) Measurement of photodegradation-caused roughness of wood using a new optical method. J Photochem Photobiol B 134:23–26. https://doi.org/10.1016/j.jphotobiol.2014.03.020

Tomak ED, Arican F, Gonultas O, Parmak EDS (2018) Influence of tannin containing coatings on weathering resistance of wood: Water based transparent and opaque coatings. Polym Degrad Stab 151:152–159

Upton BM, Kasko AM (2016) Strategies for the conversion of lignin to high-value polymeric materials: review and perspective. Chem Rev 116(4):2275–2306

Wang H, Li J, Zeng X, Tang X, Sun Y, Lei T, Lin L (2020) Extraction of cellulose nanocrystals using a recyclable deep eutectic solvent. Cellulose 27(3):1301–1314

Xu H, Peng J, Kong Y, Liu Y, Su Z, Li B, Song X, Liu S, Tian W (2020) Key process parameters for deep eutectic solvents pretreatment of lignocellulosic biomass materials: A review. Bioresour Technol 310:123416

Yang B, Zhang Q, Fei Y, Zhou F, Wang P, Deng Y (2015) Biodegradable betaine-based aprotic task-specific ionic liquids and their application in efficient SO 2 absorption. Green Chem 17(7):3798–3805

Yildiz S, Tomak ED, Yildiz UC, Ustaomer D (2013) Effect of artificial weathering on the properties of heat treated wood. Polym Degrad Stab 98(8):1419–1427

Zhang CW, Xia SQ, Ma PS (2016) Facile pretreatment of lignocellulosic biomass using deep eutectic solvents. Bioresour Technol 219:1–5